

Experiments of the Richtmyer-Meshkov Instability at High Mach Numbers using PIV

Chris Weber, Nick Haehn, Jason Oakley, Mark Anderson, & Riccardo Bonazza

University of Wisconsin-Madison
bonazza@engr.wisc.edu
<http://silver.neep.wisc.edu/~shock/>

Abstract

An abstract for an IWPCTM 12 paper should be less than 150 words. Experiments are presented for the Richtmyer-Meshkov instability of a nearly single mode interface of nitrogen over sulfur hexafluoride. The interface is created by flowing N_2 from above and SF_6 from below in a vertical shock tube. Slots at the interface location allow for a stagnation plane to form. A pair of rectangular pistons oscillate to force a nearly 2D sinusoidal standing wave. Shock waves of strength $M = 2.0$ and 2.9 accelerate the interface, depositing vorticity along the perturbation, and leading to a growth in amplitude. Due to the high Atwood number ($A = (\rho_2 - \rho_1)/(\rho_2 + \rho_1) = 0.68$) the bubble and spike grow asymmetrically with the vorticity being concentrated near the top of the spike and the bubble becoming nearly flat at later times.

Nomenclature

A	Atwood number
M	Mach number
Re	Reynolds number
TMZ	Turbulence mixing zone
α	constant in TMZ width growing
\mathbf{v}	velocity
ρ_1	density of upper fluid
ρ_2	density of lower fluid

Introduction

This article illustrates preparation of the final version of an IWPCTM 12 paper submitted for publication using $\LaTeX 2_{\epsilon}$. Template developed by Eduard Son on the basis of Template IWPCTM-10.

The full paper should be not more than 6 pages because of limitation of the whole volume around 500 pages.

As it was stated at the Conference REZUME, the author may send the paper to the peer review ASME Journal of Fluids Engineering.

You should be able to find answers to most of your questions about submitting to the journal by following this link:

<https://journaltool.asme.org/Help/AuthorHelp/WebHelp/JournalsHelp.htm>

Editorial Office (Amber Grady-Fuller).

The instability development is explored through particle image velocimetry (PIV) by seeding the nitrogen with aluminum oxide particles and acquiring a pair of planar images that are analyzed to obtain the

velocity field. The PIV data is processed to provide measurements of the vorticity distribution, circulation, and bubble/spike growth rates. An example is shown in Figure 3, which shows an interface of He/SF₆ after acceleration by a $M = 1.2$ shock wave and the vorticity field found through PIV analysis.

Since the pioneering work of Youngs [1], large eddy simulation (LES) has gained interest as a tool for predicting the turbulent variable density flows encountered in shock tube experiments.

In these experiments, the turbulent field is submitted to rapid compression and expansions, as well as large accelerations creating stable or unstable stratifications. These interactions can be strong enough to affect the small scales of turbulence and may lead to a state of rapidly distorted turbulence (RDT). On the other hand, in between interactions, turbulence is left to decay and diffuse, so that it tends to a state of spectral equilibrium.

As stressed in several works [2, 3, 4], the small scales of turbulence – and consequently the subgrid scale (SGS) model accounting for their presence in LES – behave differently whether in the RDT or in the spectral equilibrium regime.

In the spectral equilibrium limit, the small scale part of the turbulent spectrum can be shown to depend linearly on mean gradients [5]. By integrating this equilibrium spectrum, Smagorinsky-like SGS models are then obtained and justified [6]. Such derivations have essentially been applied to the context of constant density flows. An extension to stratified flows was given in [7], but with an erroneous equilibrium spectrum [5]. Besides, it seems that no derivation takes into account the effects of a mean compression/expansion.

As for the RDT limit, several studies [2, 3, 4] point out that Smagorinsky-like models fail to reproduce the main behavior of small turbulent scales. Scale-similarity and mixed models [8], on the other hand, are shown to perform better. Most of these conclusions are based on observations from experiments and direct simulations. However, they are not sustained by any theory. To the authors' knowledge, there is no derivation of a SGS model explicitly based on RDT assumptions.

Experimental Setup (Problem Formulation)

Experiments are presented for the Richtmyer-Meshkov instability of a nearly single mode interface of nitrogen over sulfur hexafluoride. The interface is created by flowing N₂ from above and SF₆ from below in a vertical shock tube. Slots at the interface location allow for a stagnation plane to form. A pair of rectangular pistons oscillate to force a nearly 2D sinusoidal standing wave. Shock waves of strength $M = 2.0$ and 2.9 accelerate the interface, depositing vorticity along the perturbation, and leading to a growth in amplitude. Due to the high Atwood number ($A = (\rho_2 - \rho_1)/(\rho_2 + \rho_1) = 0.68$) the bubble and spike grow asymmetrically with the vorticity being concentrated near the top of the spike and the bubble becoming nearly flat at later times.

Figures

There are 3 different ways to include figures into the paper text. Examples of figures see below.

1. If your figure has page size, use

```
\begin{figure}[h]
\centering\includegraphics[width=\textwidth]{weber-02.eps}
\caption{\small Setup 3}
\label{fig:weber-02}
\end{figure}
```

2. If your figure could have size less than page size, use

```
\begin{figure}[h]
\centering\epsfxsize=80mm\epsfbox{weber-01.eps}
\caption{Setup 2}
\label{fig:weber-01}
```

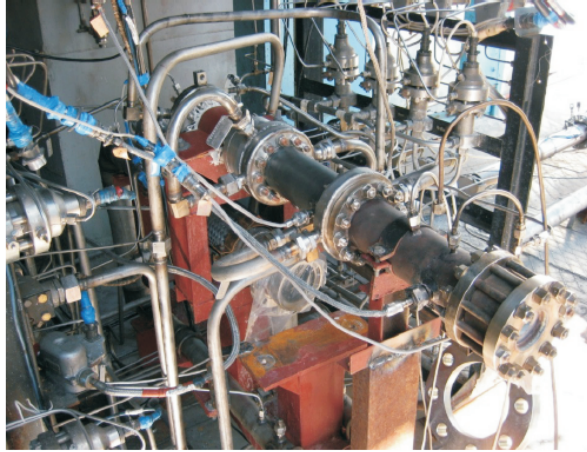


Figure 1: Experimental setup for RTI in hydrogen-fluoride flows

`\end{figure}`

3. If your figure could be small size, because it has no detailed information, use wrap mode

```
\begin{wrapfigure}[12]{1}{-10pt}{60mm}
\centering\epsfxsize=50mm\epsfbox{weber-05.eps}
\caption{\small The PIV image}
\label{fig:weber-05}
\end{wrapfigure}
```

Figure and table captions do not end with a period.

Equations

Use equation in the standard \LaTeX form (see any \TeX manual). Formula numbers should contain author name and formula number like is shown below.

$$\tau_{ij} = (\tau_0 \dot{\gamma}^{-1} + \mu_0 \dot{\gamma}^{n-1}) \dot{\gamma}_{ij}, \quad \text{for } \tau \geq \tau_0, \quad (1)$$

Tables

Use tables in the standard \LaTeX form (see any \TeX manual). Table numbers should contain author name and formula number like is shown below.

Example	Time	Cost
1	12.5	\$1,000
2	24	\$2,000

Table 1: Figure and table captions do not end with a period

All tables should be numbered consecutively and centered above the table as shown in Table 1. The body of the table should be no smaller than 7 pt. There should be a minimum two line spaces between tables and text.

Diagnostics (Numerical method)

For experimental papers describe the diagnostic methods, accuracy, errors, Company produces the equipment, etc.

For numerical simulation papers describe the solution method, accuracy, comparison with the other methods, validation

The second case also consists in an initially homogeneous and isotropic turbulence with density fluctuations, but this time subjected to an infinitely weak distortion. An asymptotic analysis of the spectral model of Canuto & Dubovikov [9] is performed in this limit. A SGS model is deduced by integrating the resulting spectra. Smagorinsky-like expressions are obtained.

Experimental Results (Results of Numerical simulation)

Simulations can provide a useful database of results for flow modelling because of the ability to acquire comprehensive statistics and measurements. Along with this, the flexibility brought by an accurate description of the conditions is particularly important when specifying $g(t)$. The code used for this work solves the incompressible Navier–Stokes equation with a second-order finite volume formulation and a multi-grid method is used to solve the Poisson equation. As standard the simulations will be carried out using $512^2 \times 1024$ grid points (double that of the Alpha-Group), but it is also possible to solve problems with up to $2048^2 \times 4096$ points.

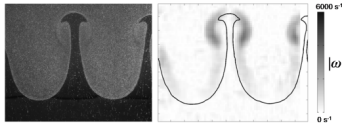


Figure 2: The image on the left shows one of the two raw PIV images while the right shows a vorticity field found through PIV analysis

Currently we have preliminary results over a range of n values from which it is possible to derive some basic statistics. The flow is self-similar when normalised measurements become constant with time and as a result the coefficient α_n will also be constant. Each of the simulations display self-similarity to a varying degree of accuracy which reduces when nearing the poles. There is a large variation in α_n particularly in the vicinity of the poles where its value increases quickly as expected, but scaling with the buoyancy-drag equation improves the collapse of the results. As with α_n other statistics are expected to vary substantially with n because the energy transfers are strongly

affected by the varying potential energy reservoir that is feeding the flow. For example when approaching the singularity with $n < -2$ the flow has increasing $g(t)$ and so becomes overloaded with directed energy, while it is expected that the energy transfer to turbulence will not keep up.

Alternatively, when the singularity is approached with $n > -2$, α_n becomes large to compensate for a rapidly decaying gravity force. The conditions in such flows are nearing that of a RM mixing layer and it is expected that there will be a corresponding change in the flow properties.

At the time of the workshop we will present full histories of statistics including input, directed and turbulent energies, along with the turbulence statistics. It may also be possible to use structure detection to separate the turbulence and large scale flow features of the mixing layer¹. Current simulations will be extended to higher Atwood number, where growth is expected to become asymmetric

Citing References

See in the \LaTeX Template file how the cites are arranged from the very beginning of this paper.

The bibliography form and list are given at the end of the paper.

Thus, the aim of this work is to derive a SGS model coherent with the RDT limit, and also with the spectral equilibrium limit when mean stratification and compression/expansion are applied. For this purpose, two idealized problems are considered, each corresponding to one of the two above mentioned asymptotic limits. In the first case, an initially homogeneous and isotropic turbulence with density fluctuations is sub-

¹R. Watteaux et al. (2010), Submitted to IWPCTM12.

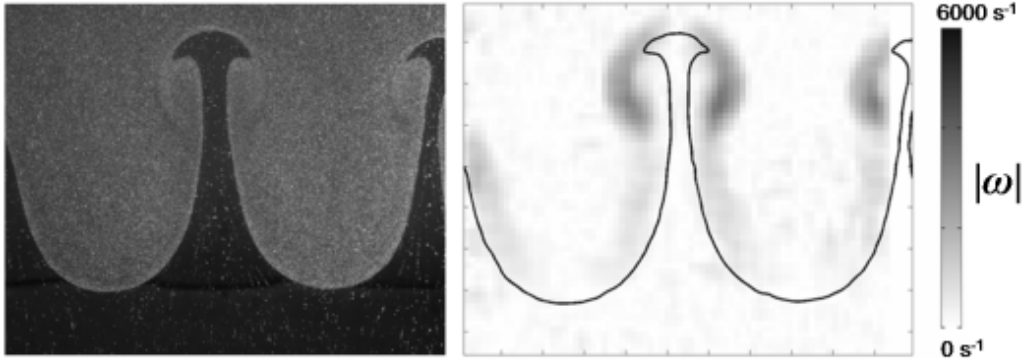


Figure 3: Post-shocked experimental image of a He/SF₆ interface after acceleration by a $M = 1.2$ shock wave. The image on the left shows one of the two raw PIV images while the right shows a vorticity field found through PIV analysis

jected to a rapid distortion. This distortion may be caused by strain, compression or stratification. A formal solution for the SGS fluxes and variances of velocity and density is established under RDT assumptions. Then, this exact solution is shown to be matched by a scale-similarity model. This scale-similarity model is different from the usual one derived in [8], as it is based on the Leonard tensor of the filtered velocity and density gradients.

The second case also consists in an initially homogeneous and isotropic turbulence with density fluctuations, but this time subjected to an infinitely weak distortion. An asymptotic analysis of the spectral model of Canuto & Dubovikov [9] is performed in this limit. A SGS model is deduced by integrating the resulting spectra. Smagorinsky-like expressions are obtained.

Conclusion

In order to validate the derived SGS model, *a priori* tests are performed with the DNS code Triclade. The first test consists in the interaction of an expansion wave with a homogeneous and isotropic mixture initially at rest. By varying the intensity of the wave, RDT conditions as well as spectral equilibrium conditions can be met. This allows to verify the two building blocks of the model independently. A second test consisting in a Rayleigh-Taylor configuration is also performed.

Discussion

Finally, the general case is treated by making a heuristic assumption. An arbitrary limit Froude number \mathcal{F}_l is introduced. Scales having a Froude number smaller than \mathcal{F}_l are assumed to be in the RDT regime. Otherwise, they are assumed to be in equilibrium. Each part of the spectrum is modeled accordingly, making use of the two SGS models derived previously. As a result, a mixed model is obtained, that naturally accounts for RDT and spectral equilibrium limits.

Acknowledgment

Thanks go to Malcolm Andrew, Antony Davies and Michail Meshkov for fruitful discussions of experimental conditions and results of LES simulation for considered problems. We would like to thank Hose

Redondo, and Matt Campbell for help in numerical simulations of our experiments. This work has been partially supported by LANL and NSF (Grant GE-2009-19-23).

References

- [1] D. Youngs. *Laser Part. Beams*, 12:725-750, 1994.
- [2] L. Shao, S. Sarkar and C. Pantano. *Phys. Fluids*, 11:1229-1248, 1999.
- [3] S. Liu, J. Katz and C. Meneveau. *J. Fluid Mech.*, 387:281-320, 1999.
- [4] J. Chen, J. Katz and C. Meneveau. *J. Fluid Eng.*, 127:840-849, 2005.
- [5] T. Ishihara, K. Yoshida, and Y. Kaneda. *Phys. Rev. Lett.*, 88:154501, 2002.
- [6] Y. Li and C. Meneveau. *Phys. Fluids*, 16:3483-3486, 2004.
- [7] A. Yoshizawa. *J. Phys. Soc. Jap.*, 52:1194-1205, 1983.
- [8] J. Bardina, J.H. Ferziger, W.C. Reynolds *AIAA paper*, 80:1357, 1980.
- [9] V.M. Canuto and M.S. Dubovikov *Phys. Fluids*, 8:571-586, 1995.